Journal of Solid State Chemistry **142,** 130–137 (1999)
Article ID jssc.1998.8000, available online at http://www.idealibrary.com on IDEAL®

Preparation and Crystal Structure of the Equiatomic Rare Earth Palladium Silicides NdPdSi, SmPdSi, α-GdPdSi, and α-TbPdSi

Yurii M. Prots' and Wolfgang Jeitschko[1]

Anorganisch-Chemisches Institut, Universität Münster, Wilhelm-Klemm-Str. 8, D-48149 Münster, Germany

Received May 18, 1998; accepted August 11, 1998

The title compounds were prepared by arc-melting of the elemental components. Whereas NdPdSi and SmPdSi are already present after the arc-melting, α-GdPdSi and α-TbPdSi are formed only during the annealing at 800°C. The four compounds crystallize with the recently reported α-YbAuGe type structure, which was refined for α-GdPdSi: *Pnma*, $a = 2108.0(4)$ pm, $b = 433.9(1)$ pm, $c = 745.6(1)$ pm, $Z = 12$, $R = 0.026$ for 1447 structure factors and 62 variable parameters. The lanthanoid atoms are situated between two-dimensionally infinite nets of condensed, puckered hexagons formed by alternating palladium and silicon atoms, with Pd–Si distances varying between 251 and 262 pm. In the third dimension these nets are linked via weak Pd–Pd (300 pm), Pd–Si (283 pm), and Si–Si bonds (261 pm). The refinements of the occupancy parameters suggested that ca. 2% of the palladium sites are occupied by silicon atoms and vice versa. The structural relationships between the two modifications of GdPdSi and the structures of AlB_2, KHg_2, TiNiSi, α-UFeGe, EuAuGe, and EuAuSn are discussed.

INTRODUCTION

Several different, but related crystal structures have been observed for equiatomic ternary rare earth palladium silicides recently. The compounds *Ln*PdSi (*Ln* = Y, Gd–Lu) crystallize with a new orthorhombic structure type, which was determined for YPdSi (1). For the large early rare earth metals lanthanum, cerium, and praseodymium, another new structure type was found, which was determined for PrPdSi (2, 3). EuPdSi, where europium is divalent, has been known for some time (4) to be isotypic with SrPdSi (4), BaPdSi (4), and LaIrSi (5). Here we report a fourth structure for equiatomic rare earth palladium silicides, which we determined for the low-temperature (α) modification of GdPdSi. It is isotypic with the most recently reported structure of α-YbAuGe (6), a centrosymmetric version of the noncentrosymmetric structure reported earlier for CaCuGe (7). This structure has recently been redetermined and found to be also centrosymmetric (8). The structures of the two modifications of GdPdSi are both superstructures of the KHg_2 type: the β-modification has a doubled cell content, and the presently reported α-modification has a tripled cell content.

SAMPLE PREPARATION, PROPERTIES, AND LATTICE CONSTANTS

The samples (~0.3 g) of the equiatomic silicides *Ln*PdSi were prepared by arc-melting of the elemental components in the ideal atomic ratio under argon. Starting materials were ingots of the rare earth elements (nominal purity 99.9%), cold-pressed pellets of palladium powder (99.9%), and pieces of high-purity silicon (6N). The neodymium and the samarium compounds were observed already in the quenched arc-melted ingots, whereas α-GdPdSi and α-TbPdSi were formed only during the annealing. At high temperatures the β-modifications of these two compounds are isotypic with YPdSi (1). For the annealing (2 weeks at 800°C) the major portion of each ingot was sealed in an evacuated silica tube. Finally the silica tubes were quenched in water. The resulting samples were microcrystalline.

The single crystals of α-GdPdSi were obtained by annealing a relatively large (0.8 g) arc-melted sample in a high-frequency furnace for 4 h slightly below its melting temperature. For this purpose the ingot was sealed in an evacuated silica tube, which was cooled on the outside with water. The thus obtained well-crystallized sample of the β-modification was then annealed for 1 month at 800°C.

The ingots of the ternary silicides show conchoidal fracture. They could also be crushed to powders; however, they are not as brittle as, for example, elemental silicon. The compact ingots as well as the powders are stable in air for long periods of time. Compact samples have metallic luster; the powders are gray.

The samples were characterized by their Guinier powder diagrams, recorded with Cu$K\alpha_1$ radiation and α-quartz ($a = 491.30$ pm and $c = 540.46$ pm) as an internal standard. All diagrams show very pronounced reflections of the body-centered, orthorhombic KHg_2 type subcell. For the

[1]To whom correspondence should be addressed.

0022-4596/99 $30.00

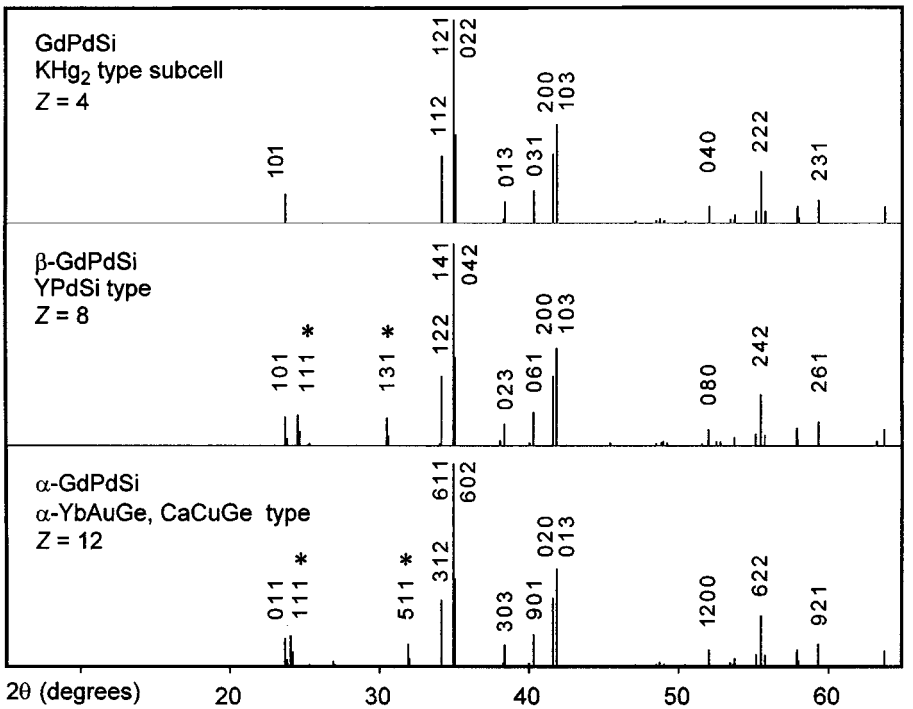

FIG. 1. Powder patterns calculated for GdPdSi and Cu$K\alpha_1$ radiation. In the top part of the figure a theoretical pattern is shown, assuming statistical distribution of palladium and silicon atoms on the mercury (copper) positions of the KHg_2 ($CeCu_2$) type structure. The other two diagrams correspond to the two superstructures observed for the two modifications of GdPdSi. The most prominent superstructure reflections are marked by asterisks. The *hkl* values of the subcell and the α-superstructure correspond to the settings as given in Table 2.

identification of the superstructure reflections, the experimentally obtained diagrams were compared with the theoretical ones, which were calculated (9) by using the positional parameters obtained during the single-crystal investigations of the α- and β-modifications of GdPdSi. As can be seen from Fig. 1, the powder diagrams of the two modifications of GdPdSi differ essentially only in the positions of two weak superstructure reflections. The lattice constants (Table 1) were refined by least-squares fits. The cell volumes per formula unit of the new compounds *Ln*PdSi (*Ln* = Nd, Sm, Gd, Tb) are similar to the corresponding values of the compounds *Ln*PdSi reported earlier (Fig. 2).

TABLE 1
Lattice Parameters of Orthorhombic Lanthanoid Palladium Silicides *Ln*PdSi with α-YbAuGe Type Structure[a]

Compound	*a* (pm)	*b* (pm)	*c* (pm)	*V* (nm^3)
NdPdSi	2156.1(4)	439.0(1)	751.9(2)	0.7117(2)
SmPdSi	2129.8(6)	436.1(1)	748.1(3)	0.6948(3)
α-GdPdSi	2108.0(4)	433.9(1)	745.6(1)	0.6820(2)
α-TbPdSi	2092.0(4)	432.2(1)	743.2(1)	0.6720(1)

[a]Standard deviations in the positions of the least significant digits are listed in parentheses throughout the paper.

STRUCTURE DETERMINATION

Small single crystals of α-GdPdSi were isolated from the crushed sample described above. They were investigated in

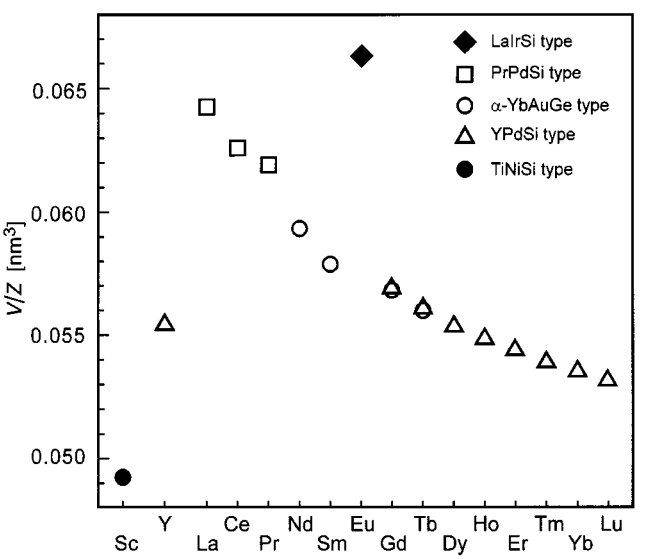

FIG. 2. Cell volumes per formula unit of equiatomic rare earth palladium silicides with different crystal structures.

TABLE 2
Crystal Data for the Subcell and the Superstructure of α-GdPdSi

Empirical formula	α-GdPdSi	
Formula mass	291.74	
Calculated density (g/cm^3)	8.52	
Crystal size (μm^3)	$30 \times 90 \times 90$	
2θ range up to (°)	75	
Maximum/minimum transmission	2.85	
	subcell	superstructure
Space group	*Imma*	*Pnma*
a (pm)	433.9(1)	2108.0(4)
b (pm)	702.7(1)	433.9(1)
c (pm)	745.6(1)	745.6(1)
V (nm^3)	0.2273(1)	0.6820(2)
Formula units/cell	$Z = 4$	$Z = 12$
Range in *hkl*	$-7 \le h \le 7$	$-36 \le h \le 36$
	$-12 \le k \le 12$	$-7 \le k \le 7$
	$0 \le l \le 12$	$0 \le l \le 12$
Total number of reflections	1168	7582
Independent reflections	342	1965
$R_{int}(F^2)$	0.049	0.053
Reflections with $I > 2\sigma$	338	1447
Variables	13	62
$R(F)$	0.022	0.026
Superstructure reflections ($I > 2\sigma$)[a]	—	1109
$R(F)$ for superstructure reflections	—	0.036
Residual peaks (e/Å^3)	−2.79/3.19	−3.39/3.34

[a]The residual for the superstructure reflections was calculated by the program RWERT (10).

a Weissenberg camera, which showed the KHg_2 type subcell and superstructure reflections corresponding to a three times larger cell with the Laue symmetry *mmm*. The space group extinctions ($0kl$ observed only with $k + l = 2n$; $hk0$ only with $h = 2n$) indicated the space groups $Pn2_1a$ and *Pnma*, of which the centrosymmetric group *Pnma* (No. 62) was found to be correct during the structure refinements.

Intensity data were collected on an Enraf-Nonius four-circle diffractometer with graphite-monochromated Mo$K\alpha$ radiation using a scintillation counter with pulse-height discrimination. The scans were along θ with background counts at both ends of each scan. An empirical absorption correction was applied from ψ-scan data. Further details are listed in Table 2.

The structure was solved with the aid of the program package SHELXS-86 (11) using direct methods, which resulted in the positions of most metal atoms. The other atomic positions were obtained by difference Fourier syntheses. The structure was refined by a full-matrix least-squares program using atomic scattering factors provided by the program package SHELXL-97 (12). The weighting scheme reflected the counting statistics, and a variable correcting for secondary extinction was fitted as a least-squares parameter. Seven very strong reflections could not be completely corrected by this fit; they were eliminated from the data set during the final least-squares cycles. This lowered the final residual from $R = 0.049$ to $R = 0.026$.

In one series of least-squares cycles the occupancy values were allowed to vary together with the anisotropic displacement parameters. No large deviations from the ideal occupancy values were observed. However, these deviations were systematic. The three palladium positions had occupancy values of slightly less than 100% and the silicon positions showed occupancy values which were slightly higher than the ideal values. For that reason we allowed mixed Pd/Si and Si/Pd occupancies for these positions in the final refinement cycles, while the occupancy values of the gadolinium positions were held constant at the ideal values. The results of these refinements are shown in Table 3. Since the amount of silicon atoms on palladium positions was approximately the same as the amount of palladium atoms on silicon positions, the composition of the investigated crystal did not differ greatly from the ideal: $Gd(Pd_{0.980(2)}Si_{0.020(2)})(Si_{0.981(2)}Pd_{0.019(2)}) = GdPd_{0.999(3)}Si_{1.001(3)}$. The positional parameters were standardized using the program STRUCTURE TIDY (13).

As discussed below, the structure of α-GdPdSi contains a very pronounced subcell of the KHg_2 type, where the position of the mercury atom is statistically occupied by palladium and silicon atoms. For comparison, this subcell has also been refined using only the (strong) subcell reflections (Table 3). The displacement parameter for this position with mixed Pd/Si occupancy, $U_{eq} = 108(2)$ pm^2, is less than double that of the average displacement parameter $\bar{U}_{eq} = 76(2)$ pm^2 of the corresponding palladium and silicon positions in the superstructure. This indicates that the positions of the palladium and silicon atoms in the superstructure do not deviate greatly from those of the subcell. Also the Pd/Si ratio of the subcell refinement is again very close to the ideal ratio 1:1 (Table 3).

TABLE 3
Atomic Coordinates and Isotropic Displacement Parameters (pm^2) for the Subcell and the Superstructure of α-GdPdSi

Atom	Occupancy	Site	x	y	z	U_{eq}
Subcell (*Imma*)						
Gd	1	4*e*	0	1/4	0.54280(4)	67(1)
Pd/Si	1.009(4)/0.991(4)	8*h*	0	0.04617(8)	0.16777(8)	108(2)
Superstructure (*Pnma*)						
Gd1	1	4*c*	0.00120(1)	1/4	0.71030(3)	65(1)
Gd2	1	4*c*	0.16613(1)	1/4	0.79618(3)	60(1)
Gd3	1	4*c*	0.33272(1)	1/4	0.70773(3)	66(1)
Pd1/Si	0.978(2)/0.022(2)	4*c*	0.09436(2)	1/4	0.42109(5)	67(1)
Pd2/Si	0.983(2)/0.017(2)	4*c*	0.23664(2)	1/4	0.41908(5)	66(1)
Pd3/Si	0.979(2)/0.021(2)	4*c*	0.43700(2)	1/4	0.41866(5)	87(1)
Si1/Pd	0.978(2)/0.022(2)	4*c*	0.07094(6)	1/4	0.0915(2)	83(4)
Si2/Pd	0.989(2)/0.011(2)	4*c*	0.27133(7)	1/4	0.0876(2)	75(4)
Si3/Pd	0.977(2)/0.023(2)	4*c*	0.39498(7)	1/4	0.0881(2)	76(4)

DISCUSSION

The equiatomic rare earth palladium silicides NdPdSi and SmPdSi are reported here for the first time. The previously characterized high-temperature (β) modifications of GdPdSi and TbPdSi have been prepared by arc-melting and they were found to be isotypic with YPdSi (1). The presently reported new low-temperature (α) modifications of these compositions were obtained during the annealing at 800°C. The phase transformations are completely reversible, as was shown by arc-melting of the α-modifications, which resulted in the β-modifications.

We determined the crystal structure of the four isotypic compounds NdPdSi, SmPdSi, α-GdPdSi, and α-TbPdSi for the gadolinium compound, which at that time appeared to be of a new centrosymmetric structure type (space group *Pnma*), which we found to be closely related to the noncentrosymmetric ($Pn2_1a$) structure reported for CaCuGe (7). However, recently the corresponding centrosymmetric structure was described also for α-YbAuGe (6). In the meantime, Kußmann and Pöttgen (8) have reinvestigated the structure of CaCuGe and they obtained a good fit of their data for the centrosymmetric group *Pnma*. Hence, it appears that CaCuGe, α-YbAuGe, and the compounds characterized in the present paper are all completely isotypic.

The refinement of the occupancy parameters of the three palladium and the three silicon positions of α-GdPdSi is of interest because it resulted in mixed occupancies of the same order of magnitude for all six positions in this sample, which had been annealed at 800°C. The greatest deviation from the ideal occupancy occurred for the Si3/Pd position with an occupancy of 0.977(2)/0.023(2) and the smallest deviation was found for the Si2/Pd position with an occupancy of 0.989(2)/0.011(2) (Table 3). These deviations from the ideal occupancies are significant because they are systematic. Nevertheless, as was shown above, the overall composition of α-GdPdSi does not significantly deviate from the ideal.

In Fig. 2 we have plotted the volumes per formula unit of all known equiatomic rare earth palladium silicides (1–4, 14, and this work). It can be seen that generally the volumes for the compounds from LaPdSi to LuPdSi follow a smooth function. An exception occurs for EuPdSi (4), where europium obviously is divalent. Small deviations from the smooth function may be due to minor errors of the lattice constant determinations by differing methods and investigators. Of the four compounds NdPdSi, SmPdSi, α-GdPdSi, and α-TbPdSi reported here, the neodymium compound and especially the samarium compound appear to have a somewhat smaller volume as expected. This might possibly be due to a slightly different composition. Samarium has a relatively high vapor pressure, which may have caused a loss of this element during the arc-melting. Nevertheless, this compound was observed practically as a single phase. The slight deviations of the lattice constants of our four compounds from the smooth function are outside the error limits of our lattice constant determinations and therefore they indicate (minor) homogeneity ranges.

Obviously, for the trivalent rare earth elements the size of the rare earth atom is the most important factor determining the structure (Fig. 2). With the large, early rare earth elements, the compounds adopt the PrPdSi type structure (3). They are followed by the compounds of the present paper. The small, late lanthanoids form compounds which are isotypic with YPdSi (1), and the still smaller scandium atom is found in ScPdSi (14), which is isotypic with TiNiSi (15) and TiPdSi (16). The largest cell volume per formula unit is observed for EuPdSi (4) with the LaIrSi type structure (5). This is also the compound where the rare earth atom (Eu) has the highest coordination number (CN), with seven palladium, seven silicon, and six europium neighbors (CN 20). In the PrPdSi type compounds, one praseodymium atom has CN 20 (5Pd + 7Si + 8Pr), while the other has CN 18 (7Pd + 5Si + 6Pr). The three remaining structure types do not differ that much in the coordination of the rare earth atoms. In all of them the rare earth atoms have six palladium and six silicon neighbors. In addition, they have four rare earth atoms as neighbors with two additional ones somewhat further away.

The structure of α-GdPdSi may be considered as an anionic network of palladium and silicon atoms in which the electropositive gadolinium atoms are embedded. The network is best described as consisting of six-membered rings of alternating palladium and silicon atoms. These rings are condensed, thus forming two-dimensionally infinite nets. Two slightly differently puckered nets are formed, designated with the letters a and b in Fig. 3. In the projections on the left-hand side of this figure, the puckering is slightly exaggerated. A more realistic picture of the puckering can be obtained from Fig. 4, which shows the environments of the three different gadolinium positions.

Two kinds of interfaces exist between the two-dimensionally infinite palladium–silicon nets. They are shown on the right-hand side of Fig. 3, designated with the letters A and B. The three palladium–silicon bonds per atom within the two-dimensional nets have bond lengths varying between 250.7 and 261.9 pm (Table 4). Each of these palladium and silicon atoms has a fourth neighbor, completing a distorted tetrahedron, which belongs to the nets above or below. These bonds are weaker, with Pd–Pd, Pd–Si, and Si–Si bond lengths of 299.9, 282.5, and 260.7 pm, respectively. These distances are all greater than the sums of the corresponding tetrahedral radii of 256.6, 245.6, and 234.6 pm, respectively, given by Pauling (17). In addition to these palladium–silicon interactions, each palladium and each silicon atom has six gadolinium neighbors, with Pd–Gd bond lengths varying between 291.7 and 320.4 pm and Si–Gd bond lengths varying between 296.2 and 321.4 pm.

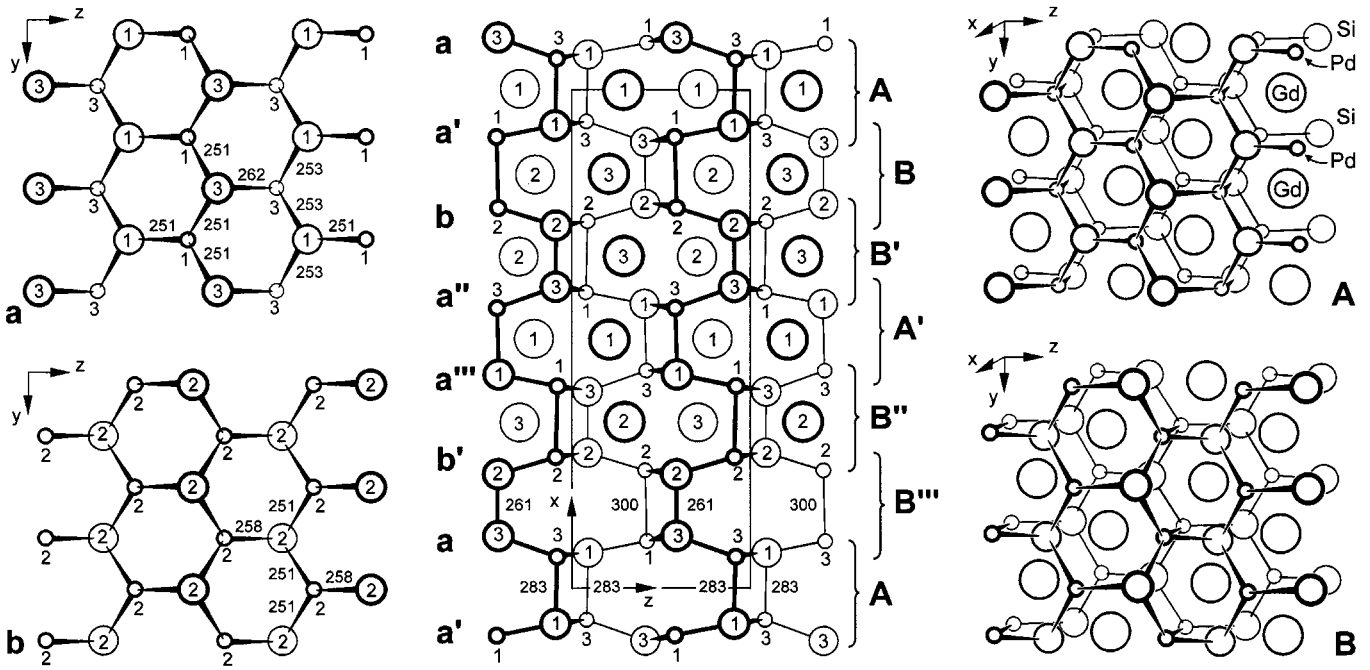

FIG. 3. Crystal structure of α-GdPdSi emphasizing the bonding within the polyanionic palladium–silicon network. In the middle of the figure the structure is projected parallel to the short *b* axis of the orthorhombic cell. The structure may be thought to consist of two-dimensionally infinite puckered palladium–silicon nets of the type a and b. These are shown in projections perpendicular to the nets on the left-hand side of the figure. Two different kinds of interfaces A and B exist between these nets, as is shown on the right-hand side. Single-digit numbers correspond to the atom designations; interatomic distances are indicated in pm units.

The two different kinds of interfaces A and B shown in Fig. 3 differ in that the interface A has only (weak) heteronuclear (Pd–Si) bonds, whereas the interface B has only (weak) homonuclear (Pd–Pd and Si–Si) bonds. Such puckered nets of palladium and silicon atoms also occur in the TiNiSi type structure of ScPdSi and in the YPdSi type compounds (1, 18). In ScPdSi only the interface A is observed, in the YPdSi type compounds the interfaces A and B alternate, and here in the palladium silicides with the α-YbAuGe (CaCuGe) type structure these interfaces occur in the sequence ABB, ABB (Fig. 3). The gold and germanium atoms of EuAuGe (19) form similar puckered hexagonal nets; there only the homonuclear interface of the type B is found.

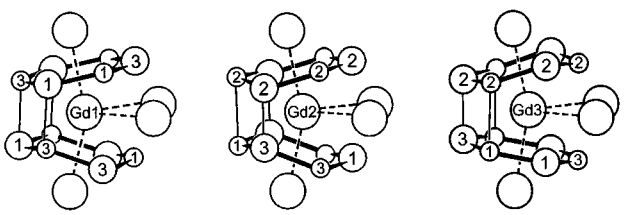

FIG. 4. Near-neighbor environments of the three gadolinium sites in α-GdPdSi.

In Fig. 5 we show the structure of α-GdPdSi together with the closely related structure of β-GdPdSi (1) and the TiNiSi type structure, which occurs for ScPdSi (14). These three structures can be derived from the well-known hexagonal AlB_2 type structure, which is shown here in an unusual projection along the hexagonal *b* axis to emphasize its relationship to the other structures. In the orthorhombic structure of KHg_2 (20), frequently also designated the $CeCu_2$ (21) type structure, the hexagonal *c* axis of the AlB_2 type structure is doubled. In the TiNiSi type structure of ScPdSi the palladium and silicon atoms occupy the mercury positions of KHg_2 in an ordered manner. In the structures of β- and α-GdPdSi the translation periods corresponding to the hexagonal axis of AlB_2 are four and six times larger, allowing more complicated stackings for the palladium and silicon atoms filling the hexagonal prisms formed by the gadolinium atoms (which correspond to the aluminum atoms of AlB_2). The space group relationships and the correspondence of the atomic positions of these structures (with the exception of AlB_2) are shown in Fig. 6.

In borides, silicides, and phosphides the metalloid atoms (boron, silicon, and phosphorus) are frequently located in trigonal prisms of metal atoms, which are augmented by three additional neighbors (metal and/or metalloid atoms) outside the rectangular faces of the prisms (22, 23). This is also the environment of the silicon atoms in

TABLE 4
Interatomic Distances in α-GdPdSi[a]

Gd1:	1Pd1	291.7	Gd3:	1Pd2	295.5	Pd3:	2Si1	252.9
	2Pd3	296.9		2Pd2	305.4		1Si3	261.9
	2Si1	303.4		1Pd3	307.9		1Si1	282.5
	1Pd3	308.0		2Si1	309.5		2Gd1	296.9
	2Pd1	311.9		2Pd1	309.8		1Gd3	307.9
	1Si3	315.7		1Si2	311.4		1Gd1	308.0
	1Si1	320.0		1Si3	312.5		2Gd2	320.4
	2Si3	321.4		2Si2	321.2	Si1:	1Pd1	250.7
	1Gd2	353.5		1Gd2	357.3		2Pd3	252.9
	1Gd3	360.4		1Gd1	360.4		1Pd3	282.5
	2Gd1	381.4		2Gd2	375.8		1Gd2	297.9
Gd2:	2Si3	296.2	Pd1:	1Si1	250.7		2Gd1	303.4
	2Si2	297.7		2Si3	251.2		2Gd3	309.6
	1Si1	297.9		1Gd1	291.7		1Gd1	320.0
	1Si2	310.5		1Pd2	299.9	Si2:	2Pd2	251.3
	2Pd2	312.2		2Gd3	309.8		1Pd2	257.7
	1Pd1	318.0		2Gd1	311.9		1Si3	260.7
	1Pd2	318.0		1Gd2	318.0		2Gd2	297.7
	2Pd3	320.4	Pd2:	2Si2	251.3		1Gd2	310.5
	1Gd1	353.5		1Si2	257.7		1Gd3	311.4
	1Gd3	357.3		1Gd3	295.6		2Gd3	321.2
	2Gd3	375.8		1Pd1	299.9	Si3:	2Pd1	251.2
				2Gd3	305.4		1Si2	260.7
				2Gd2	312.2		1Pd3	261.9
				1Gd2	318.0		2Gd2	296.2
							1Gd3	312.5
							1Gd1	315.7
							2Gd1	321.4

[a]All distances shorter than 390 pm (Gd–Gd, Gd–Pd, Gd–Si) and 360 pm (Pd–Pd, Pd–Si, Si–Si), respectively, are listed. Standard deviations are all less than 0.3 pm.

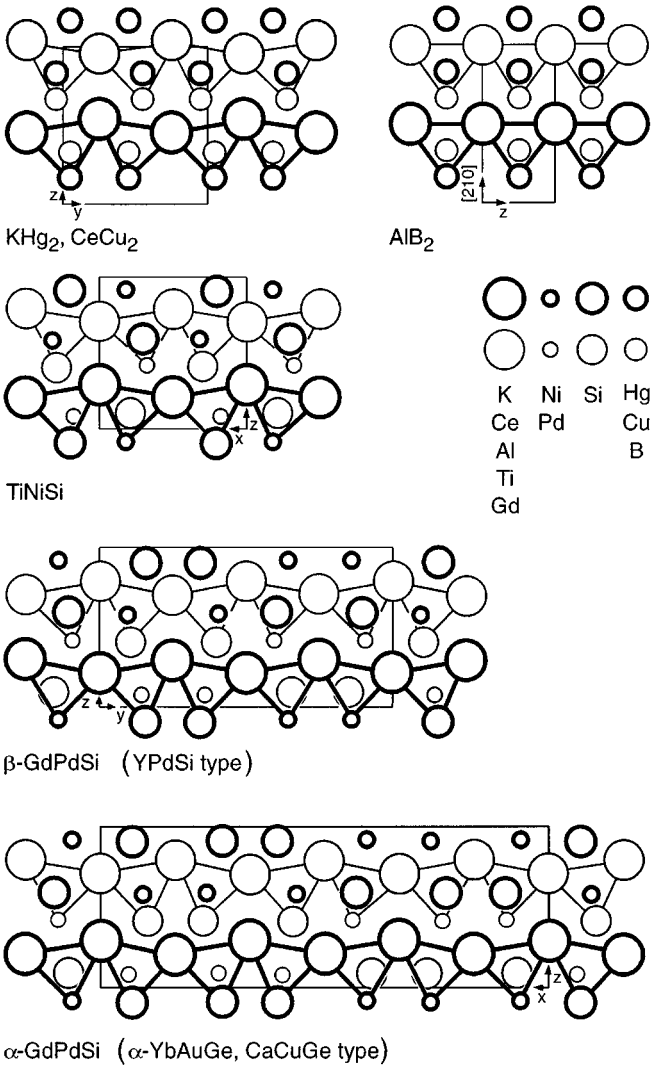

FIG. 5. Crystal structures of α- and β-GdPdSi as compared to the structures of TiNiSi, KHg_2, and AlB_2. The structures are projected along a short translation period. Certain trigonal prisms forming chains in these projections are emphasized to show similarities. In the structure of TiNiSi these prisms are filled with nickel and silicon atoms in the sequence NiSi, NiSi. In α- and β-GdPdSi the corresponding sequences are PdPdSiSi, PdPdSiSi and PdPdPdSiSiSi, PdPdPdSiSiSi, respectively.

α- and β-GdPdSi, except that the silicon atoms are shifted slightly out of the centers of the trigonal prisms, in this way obtaining a tenth neighbor. Thus, there are two neighbors outside one of the rectangular faces of the trigonal prism instead of one.

Frequently the arrangements of the trigonal prisms around the silicon atoms are used to classify the structures of silicides [e.g., (24) and (25)]. In the structures of α- and β-GdPdSi, trigonal prisms are found not only around the silicon atoms but also around the palladium atoms, again with a total of four additional neighbors outside the rectangular faces of the prisms. In agreement with previous discussions on related structures (1, 26), we emphasize in Fig. 7 the trigonal prisms around the transition metal atoms. It can be seen that these trigonal prisms form chains in the projection (considering the three-dimensional character of these structures, the chains correspond to layers, since the trigonal prisms share their triangular faces with the prisms above and below). These chains extend from the left to the right in Fig. 7. The nonconnected edges of the prisms point up (+) or down (−) the z direction of all structures. In this way the structures can be classified with, for example, the sequence $--++$, $--++$ and $---+++$, $---+++$ for β- and α-GdPdSi. Since both the palladium and the silicon atoms correspond to boron atoms of the prototype AlB_2 (Fig. 5), the same sequence is also obtained if the orientation of the trigonal prisms around the silicon atoms is used for the classification.

It has frequently been discussed that the high-temperature modification of a solid-state compound has a higher symmetry structure than the low-temperature modification, or at least the low-temperature modification requires a larger number of positional parameters for its description. This

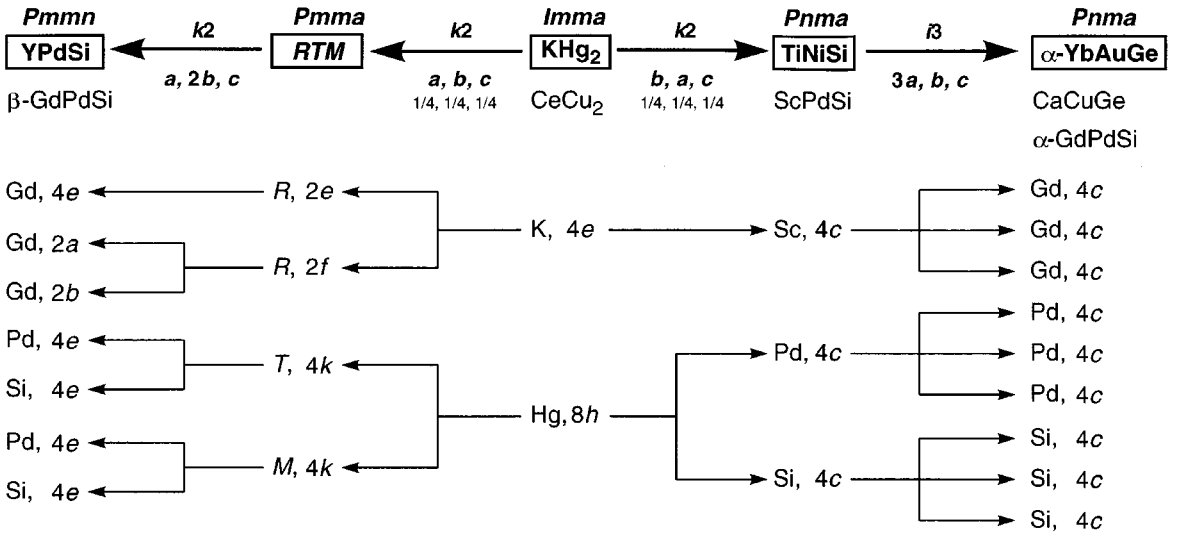

FIG. 6. Space group relationships and correspondence of the occupied Wyckoff positions of the two modifications of GdPdSi and related structures, including the hypothetical structure *RTM*.

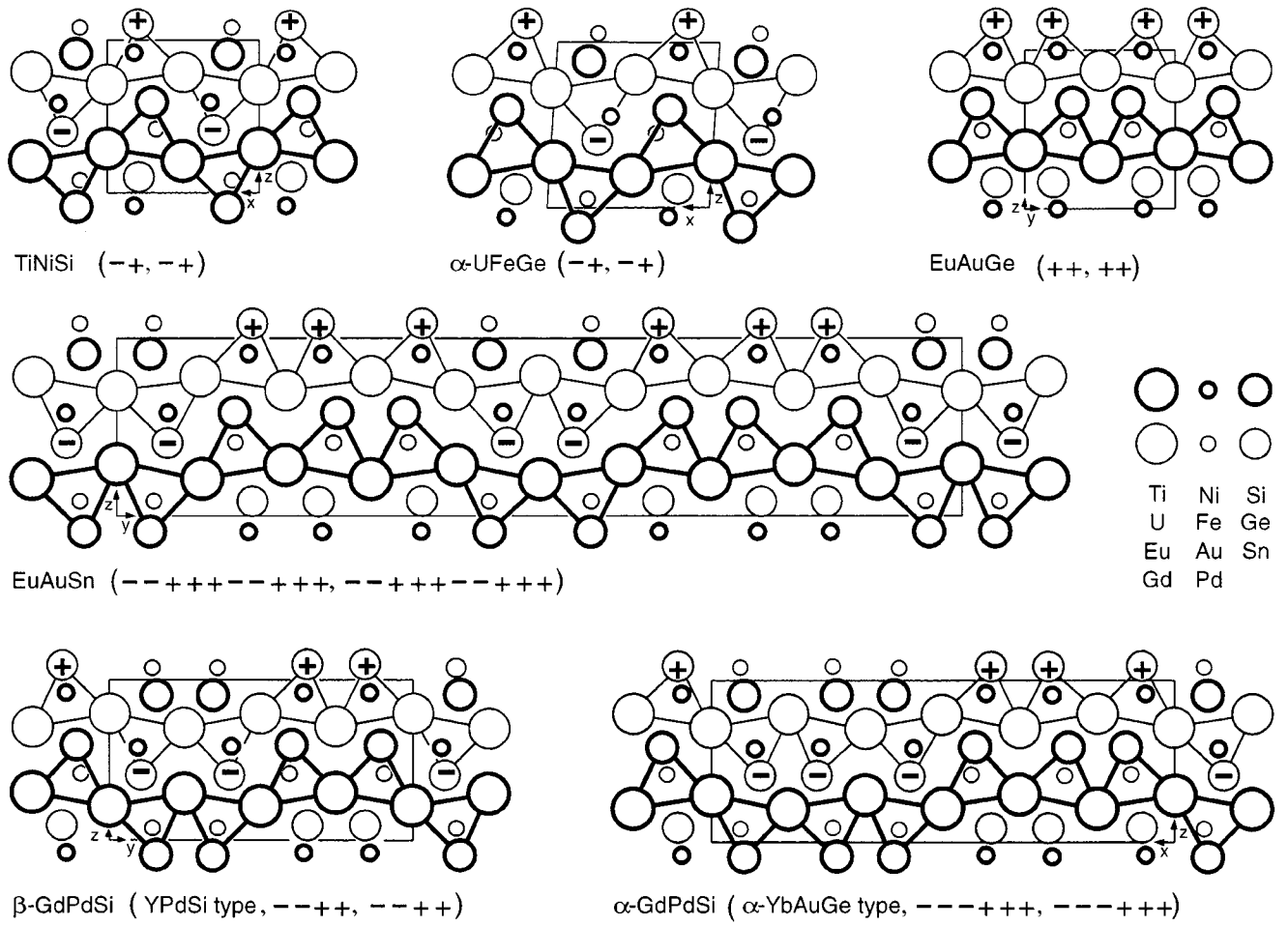

FIG. 7. Crystal structures of the four compounds TiNiSi (15), α-UFeGe (27), EuAuGe (19), and EuAuSn (26) as compared to the structures of the two modifications of GdPdSi. The projections are along the shortest axes. All atoms are situated on mirror planes, which extend perpendicular to the short axes. The trigonal prisms around the transition metal atoms are emphasized. The orientations of the silicon, germanium, and tin edges of the trigonal prisms are indicated by the symbols + and −.

is also the case for the structures of β- and α-GdPdSi. Their space groups (*Pmmn* and *Pnma*) have the same crystal class, both with eightfold general positions. However, since the unit cell of the low-temperature (α) modification is larger, the atoms of this modification occupy more atomic sites (nine, Fig. 6) than the atoms of the high-temperature (β) modification (seven) with a corresponding difference of variable positional parameters.

ACKNOWLEDGMENTS

We are grateful to Dipl.-Ing. U. Ch. Rodewald for the intensity data collection and to K. Wagner for the investigations at the scanning electron microscope. We also thank Dr. G. Höfer (Heraeus Quarzschmelze) for a generous gift of silica tubes and Dr. W. Gerhartz (Degussa) for palladium powder. Yu.M.P. is indebted to the DAAD and the Heinrich Hertz-Stiftung for research stipends. This work was also supported by the Fonds der Chemischen Industrie and the Deutsche Forschungsgemeinschaft.

REFERENCES

1. Yu. M. Prots', R. Pöttgen, and W. Jeitschko, *Z. Anorg. Allg. Chem.* **624,** 425 (1998).
2. Yu. M. Prots' and W. Jeitschko, *Z. Kristallogr. Suppl.* **12,** 138 (1997).
3. Yu. M. Prots', M. Gerdes, and W. Jeitschko, *Z. Anorg. Allg. Chem.* **624,** 1855 (1998).
4. J. Evers, G. Oehlinger, K. Polborn, and B. Sendlinger, *J. Solid State Chem.* **91,** 250 (1991).
5. K. Klepp and E. Parthé, *Acta Crystallogr., Sect. B* **38,** 1541 (1982).
6. F. Merlo, M. Pani, F. Canepa, and M. L. Fornasini, *J. Alloys Compd.* **264,** 82 (1998).
7. W. Dörrscheidt, N. Niess, and H. Schäfer, *Z. Naturforsch., B* **32,** 985 (1997).
8. D. Kußmann and R. Pöttgen, *Z. Kristallogr. Suppl.* **15,** 52 (1998).
9. K. Yvon, W. Jeitschko, and E. Parthé, *J. Appl. Crystallogr.* **10,** 73 (1977).
10. R.-D. Hoffmann, RWERT, Program for the Calculation of Separate Residuals for Superstructure Reflections, Univ. Münster, 1996.
11. G. M. Sheldrick, SHELXS-86, Program for Crystal Structure Determination, Univ. Göttingen, Göttingen, Germany, 1986.
12. G. M. Sheldrick, SHELXL-97, Program for Crystal Structure Refinement, Univ. Göttingen, Göttingen, Germany, 1997.
13. L. M. Gelato and E. Parthé, *J. Appl. Crystallogr.* **20,** 139 (1987).
14. E. Hovestreydt, N. Engel, K. Klepp, B. Chabot, and E. Parthé, *J. Less-Common Met.* **85,** 247 (1982).
15. C. B. Shoemaker and D. P. Shoemaker, *Acta Crystallogr.* **18,** 900 (1965).
16. V. Johnson and W. Jeitschko, *J. Solid State Chem.* **4,** 123 (1972).
17. L. Pauling, *in* "The Chemical Bond," p. 150. Cornell Univ. Press, Ithaca, NY, 1967.
18. Yu. M. Prots', R. Pöttgen, D. Niepmann, M. W. Wolff, and W. Jeitschko, *J. Solid State Chem.* (in press).
19. R. Pöttgen, *J. Mater. Chem.* **5,** 505 (1995).
20. E. J. Duwell and N. C. Baenziger, *Acta Crystallogr.* **8,** 705 (1955).
21. A. C. Larson and D. T. Cromer, *Acta Crystallogr.* **14,** 73 (1961).
22. B. Aronsson, *Ark. Kemi* **16,** 379 (1960).
23. S. Rundqvist, *Ark. Kemi* **20,** 67 (1962).
24. E. I. Gladyshevskii and Yu. N. Grin', *Sov. Phys. Crystallogr.* **26,** 683 (1981).
25. E. Parthé and B. Chabot, *in* "Handbook on the Physics and Chemistry of Rare Earths" (K. A. Gschneidner, Jr., and L. Eyring, Eds.), Vol. 6, pp. 113–334. North-Holland, Amsterdam, 1984.
26. R. Pöttgen, R.-D. Hoffmann, R. Müllmann, B. D. Mosel, and G. Kotzyba, *Chem. Eur. J.* **3,** 1852 (1997).
27. F. Canepa, P. Manfrinetti, M. Pani, and A. Palenzona, *J. Alloys Compd.* **234,** 225 (1996).